

Off-shell  $\rho$ - $\omega$  mixing in QCD sum rulesT. Hatsuda,<sup>1,\*</sup> E. M. Henley,<sup>1,2,†</sup> Th. Meissner,<sup>2,‡</sup> and G. Krein,<sup>3,§</sup><sup>1</sup> *Physics Department, FM-15, University of Washington, Seattle, Washington 98195*<sup>2</sup> *Institute for Nuclear Theory, HN-12, University of Washington, Seattle, Washington 98195*<sup>3</sup> *Instituto de Física Teórica, Rua Pamplona, 145, 01405-900 São Paulo-SP, Brazil*

(Received 26 April 1993)

The  $q^2$  dependence of the  $\rho$ - $\omega$  mixing amplitude is analyzed with the use of QCD sum rules and dispersion relations. Going off shell the mixing decreases, changes sign at  $q^2 \simeq 0.4m_\rho^2 > 0$ , and is negative in the spacelike region. Implications of this result for the isospin breaking part of the nuclear force are discussed.

PACS number(s): 24.85.+p, 13.75.Cs, 14.40.Cs, 11.55.Hx

## I. INTRODUCTION

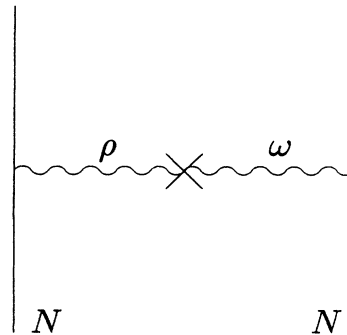
Although charge independence and charge symmetry are respected approximately by the strong interactions, these symmetries are both broken by the electromagnetic interaction and the mass difference of the up and down quarks. The symmetry breaking remains of considerable interest both experimentally and theoretically because it can be studied by perturbation theory. At low energies, the large scattering length of two nucleons in the  $^1S_0$  state makes it particularly suitable for investigations of both charge independence and charge symmetry [1]. At medium energies, polarization experiments in  $n$ - $p$  scattering have been of interest for studies of charge symmetry [2,3]. In nuclei, the mass difference between light-to-medium conjugate nuclear pairs (with a neutron replaced by a proton) also shows charge symmetry breaking beyond that due to Coulomb forces; this is commonly referred to as the Nolen-Schiffer or Okamoto-Nolen-Schiffer anomaly [4,5].

Theoretically, charge-dependent forces have been cast into four classes [6]. It is the class IV forces, proportional to  $(\tau_1^{(3)} - \tau_2^{(3)})$  and  $(\tau_1 \times \tau_2)^{(3)}$ , where  $\tau_i^j$  is the  $j$ th component of the Pauli isospin matrix for particle  $i$ , which produce charge-symmetry-breaking effects in the  $n$ - $p$  system. In meson-theoretic investigations [7], these forces are due to (in addition to photon exchange) pion exchange, mixed  $\rho$ - $\omega$  and  $\pi$ - $\eta$ - $\eta'$  exchanges, combined  $\pi$ - $\gamma$  and other complex exchanges. The experimental asymmetries measured at 477 MeV [2] and 183 MeV [3] are particularly sensitive to pion exchange and  $\rho$ - $\omega$  mixed exchange, respectively. Indeed, both experiments agree with theoretical predictions based on meson theory [7].

At 183 MeV, the dominant contribution to the polarization asymmetry in the  $n$ - $p$  elastic scattering cross section is found to arise from  $\rho$ - $\omega$  mixing in the exchanged

mesons, as shown in Fig. 1. However, it has been pointed out by Goldman, Henderson, and Thomas [8] that the fit makes use of the on-mass-shell mixing of  $\rho$  and  $\omega$ , as measured in  $e^+e^-$  collisions, whereas it is space-like values of the four-momentum transfer ( $q^2 < 0$ ) that are required for the fit to the  $n$ - $p$  scattering data. Furthermore, they point out that in a model which uses free quark-antiquark intermediate states, there is considerable variation of the rho-omega mixing parameter with  $q^2$ ; indeed, it changes sign at  $q^2 \sim -(400 \text{ MeV})^2$  and is small for negative (spacelike) values of  $q^2$ . This casts doubt on the theoretical calculations [7]. More recently, Piekarewicz and Williams [9] have used an intermediate  $N\bar{N}$  to calculate the mixing and obtain qualitatively similar conclusions to Goldman *et al.*

The Nolen-Schiffer anomaly has also seen a revival of interest. In a meson-theoretic investigation, the type-III forces proportional to  $(\tau_1^{(3)} + \tau_2^{(3)})$ , in particular the  $\rho$ - $\omega$  mixing contribution, is claimed to be an essential ingredient to explain the anomaly [10]. However, the on-mass-shell value of the  $\rho$ - $\omega$  mixing is also used in this analysis. The partial restoration of chiral symmetry in nuclei and the associated change of the  $n$ - $p$  mass difference in medium is another explanation of the anomaly without recourse to rho-omega mixing [11]. The effective theory of QCD [11] and QCD sum rules in a nuclear medium [12] seem to support this explanation. Further

FIG. 1. Class III and IV nuclear force from the  $\rho$ - $\omega$  mixing.

\*Internet address: hatsuda@diana.ph.tsukuba.ac.jp

†Internet address: henley@alpher.npl.washington.edu

‡Internet address: meissner@ben.npl.washington.edu

§Internet address: gkrein@ift.uesp.ansp.br

extension of the approach in Ref. [12] is also made by taking into account the mixing in the vector channel [13]. Thus it is important to find out the relative importance of  $\rho$ - $\omega$  mixing among other explanations by analyzing the  $q^2$  variation of the mixing.

Of the various nonperturbative approaches in QCD, QCD sum rules have been found to be a powerful tool for analyzing the properties and decays of hadrons [14,15]. They can give a plausible explanation of the Nolen-Schiffer anomaly [12] as we mentioned above. One of the earliest applications of the sum rules was actually to a calculation of the on-mass-shell  $\rho$ - $\omega$  mixing [16].

In this paper, we follow the path forged by Shifman, Vainshtein, and Zakharov (SVZ) [16], but we extend it to spacelike values of  $q^2$  which is the relevant region of the charge-dependent nuclear forces. Furthermore, we reevaluate the various semiphenomenological constants required by the sum rules. Whereas SVZ used a value of  $\beta$  (see below) obtained from a ‘‘speculation’’ based on ‘‘the experience with sum rules,’’ or as a free parameter, we obtain  $\beta$  from the sum rules themselves. In Sec. II, we will summarize the effect of the  $\rho$ - $\omega$  mixing on the nuclear force and give an essential idea about the importance of the  $q^2$  dependence of the mixing. In Sec. III, we will determine the parameters which control the  $q^2$  varia-

tion from QCD sum rules. The combined use of the Borel sum rules and the finite energy sum rules together with the current knowledge of the quark mass difference and the quark condensates give us an unambiguous determination of these parameters without further assumptions. We find that some of the outputs are different in magnitude and sign from the SVZ results. In Sec. IV, the  $q^2$  dependence of the  $\rho$ - $\omega$  mixing and also its effect on the nuclear force are discussed by using the parameters determined in Sec. III. The mixing amplitude  $\theta(q^2)$  changes sign at  $q^2 \simeq 0.4m_\rho^2$  and gets negative in the space-like region, which is qualitatively consistent with the previous analysis [8,9]; however the effect is stronger in our case. In coordinate space, this corresponds to a node of the charge-dependent potential around  $r \simeq 0.9$  fm which suppresses the effect of the  $\rho$ - $\omega$  mixing in the nuclear force. Section V is devoted to a summary and concluding remarks.

## II. $\rho$ - $\omega$ MIXING IN THE SPACELIKE REGION

The Feynman graph for the class III and IV forces originating from  $\rho$ - $\omega$  mixing is shown in Fig. 1. The cross in Fig. 1 denotes the  $\rho$ - $\omega$  mixing  $\theta(q^2)$  defined in terms of the mixed propagator

$$\begin{aligned} \Pi_{\mu\nu}^{\rho\omega}(q^2) &= i \int d^4x e^{iqx} \langle T \rho_\mu(x) \omega_\nu(0) \rangle_0 \\ &= (-) \left( g_{\mu\nu} - \frac{q_\mu q_\nu}{q^2} \right) \frac{\theta(q^2)}{(q^2 - m_\rho^2 + i\epsilon)(q^2 - m_\omega^2 + i\epsilon)}, \end{aligned} \quad (2.1)$$

where we have neglected the width of the resonances for simplicity.

At  $q^2 = m_\omega^2$ ,  $\theta(q^2)$  reduces to the mixing matrix  $\langle \rho | H_{\text{SB}} | \omega \rangle$  measured in the  $e^+e^- \rightarrow \pi^+\pi^-$  data [17]

$$\begin{aligned} \theta(q^2 = m_\omega^2) &= \langle \rho | H_{\text{SB}} | \omega \rangle \\ &= (-4520 \pm 600) \text{ MeV}^2. \end{aligned} \quad (2.2)$$

Here  $H_{\text{SB}}$  is a part of the Hamiltonian which breaks isospin symmetry and we have used the covariant definition of the mixing matrix  $\langle \rho_\mu | H_{\text{SB}} | \omega_\nu \rangle = -(g_{\mu\nu} - q_\mu q_\nu / q^2) \langle \rho | H_{\text{SB}} | \omega \rangle$  following Ref. [18].

$H_{\text{SB}}$  has both QED and QCD origins. One of the QED effects to Eq. (2.1), from  $\rho \rightarrow \gamma \rightarrow \omega$ , can be explicitly calculated and gives a small and positive contribution [19]:

$$\theta_{\rho \rightarrow \gamma \rightarrow \omega}(m_\omega^2) = \frac{e^2}{m_\rho^2 g_\rho g_\omega} \simeq 610 \text{ MeV}^2, \quad (2.3)$$

where  $e/g_\rho$  and  $e/g_\omega$  denote, respectively, the electromagnetic coupling of  $\rho$  and  $\omega$  with  $\gamma$ . We have assumed  $g_\omega \simeq 3g_\rho$ , as obtained from the flavor SU(3) symmetry. Thus the main part of the observed mixing comes from the quark mass difference

$$m_d - m_u \simeq 0.28(m_d + m_u), \quad (2.4)$$

where  $(m_d + m_u)/2 = (7 \pm 2) \text{ MeV}$  at a 1 GeV QCD scale ([20] and references therein). Note also that, once one takes into account the  $\gamma$  exchange between nucleons with proper nucleon electromagnetic form factors (Fig. 2), one has to subtract the  $\rho \rightarrow \gamma \rightarrow \omega$  effect from Fig. 1 to avoid double counting. (The QED mixing is hidden in the form factors in Fig. 2.)

For isospin mixing in the nuclear force, we are concerned with spacelike momenta  $q^2 < 0$ , which is far from the on-shell point  $q^2 = m_{\rho,\omega}^2$ . Thus it is crucial to study the  $q^2$  variation of  $\theta(q^2)$  to determine whether one can naively utilize the on-shell mixing value, Eq. (2.2), in the spacelike region [8]. In the next section, we will analyze the  $q^2$  variation of  $\rho$ - $\omega$  mixing on the basis of the QCD sum rules in which the physical quantities are related to the condensates in the QCD vacuum. Our approach has less ambiguities compared to other approaches based on phenomenological models [8,9]. Before entering into details, let us discuss the primary origin of the  $q^2$  variation to demonstrate the essential idea in a model-independent way.

We start with the unsubtracted dispersion relation for the polarization operator  $\Pi_{\mu\nu}^{\rho\omega}(q^2) \equiv (-)(g_{\mu\nu} - \frac{q_\mu q_\nu}{q^2}) \Pi^{\rho\omega}(q^2)$ :

$$\text{Re} \Pi^{\rho\omega}(q^2) = \frac{\text{P}}{\pi} \int_0^\infty \frac{\text{Im} \Pi^{\rho\omega}(s)}{s - q^2} ds. \quad (2.5)$$

If  $q^2$  is not too large and in the spacelike region, the main contribution to  $\text{Re}\Pi_{\mu\nu}^{\rho\omega}$  comes from the lowest poles in the imaginary part of  $\Pi_{\mu\nu}^{\rho\omega}$ , i.e., the  $\rho$  and  $\omega$  resonances. It is important to note that for the mixing,  $\Pi_{\mu\nu}^{\rho\omega}$ , unlike the case for  $\Pi_{\mu\nu}^{\rho\rho}$ , the integral of the continuum contribution such as that from an  $N\bar{N}$  loop is finite [9]. If photon exchange is included in the loop, this is no longer the case; however, by carrying out the Borel analyses in the

QCD sum rule, we find this contribution to the mixing is to be small numerically ( $\approx 2\%$ ), so that it can be neglected (see Sec. III for more details). Thus we do not need any subtraction on the right-hand side of Eq. (2.5) as far as the strong interaction is concerned. In the pole approximation,  $\text{Im}\Pi_{\mu\nu}^{\rho\omega}(s)$  is easily evaluated by saturating the intermediate states by  $\rho$  and  $\omega$  mesons:

$$\begin{aligned} \text{Im}\Pi_{\mu\nu}^{\rho\omega}(s) &= \pi\langle 0|\rho_\mu|\rho\rangle\langle\rho|\omega_\nu|0\rangle\delta(s-m_\rho^2) + \pi\langle 0|\rho_\mu|\omega\rangle\langle\omega|\omega_\nu|0\rangle\delta(s-m_\omega^2) \\ &\equiv (-)\left(g_{\mu\nu} - \frac{q_\mu q_\nu}{q^2}\right) [\pi F_\rho\delta(s-m_\rho^2) - \pi F_\omega\delta(s-m_\omega^2)]. \end{aligned} \quad (2.6)$$

It is not difficult to see that the pole residues  $F_\rho$  and  $F_\omega$  in Eq. (2.6) are proportional to  $(m_d - m_u)/(m_\omega^2 - m_\rho^2)$  in QCD. Also, they do not have to be equal [16]

$$F_\rho \neq F_\omega. \quad (2.7)$$

Substituting (2.6) into (2.5), one obtains

$$\begin{aligned} \text{Re}\Pi_{\mu\nu}^{\rho\omega}(q^2) &= (-)\left(g_{\mu\nu} - \frac{q_\mu q_\nu}{q^2}\right) \left[ \frac{-F_\rho}{q^2 - m_\rho^2} + \frac{F_\omega}{q^2 - m_\omega^2} \right] \\ &= (-)\left(g_{\mu\nu} - \frac{q_\mu q_\nu}{q^2}\right) \frac{(+\delta m^2)(F_\rho + F_\omega)/2 - (q^2 - m^2)(F_\rho - F_\omega)}{(q^2 - m_\rho^2)(q^2 - m_\omega^2)}, \end{aligned} \quad (2.8)$$

where  $m^2 \equiv (m_\rho^2 + m_\omega^2)/2$  and  $\delta m^2 \equiv m_\omega^2 - m_\rho^2$ .

Thus we finally get

$$\theta(q^2) = \theta(m^2) \left[ 1 + \lambda \left( \frac{q^2}{m^2} - 1 \right) \right], \quad (2.9)$$

with  $\theta(m^2) = (+\delta m^2)(F_\rho + F_\omega)/2$  and  $\lambda = -(F_\rho - F_\omega)m^2/\theta(m^2)$ . The first term of Eq. (2.8) is nothing but the usual on-shell mixing matrix  $\langle\rho|H_{\text{SB}}|\omega\rangle$ , while the second term gives a  $q^2$  variation due to  $F_\rho \neq F_\omega$ . Since both the first and second terms are proportional to  $m_d - m_u$  and are of the same order, there is no *a priori* reason to neglect the second term. However, in most phenomenological applications [1,7,10] of  $\rho$ - $\omega$  mixing to the charge-symmetry-breaking nuclear force,  $F_\rho = F_\omega$  has been assumed without any justification. For instance, a  $q^2$  dependence of  $\rho$ - $\omega$  mixing was considered in Ref.

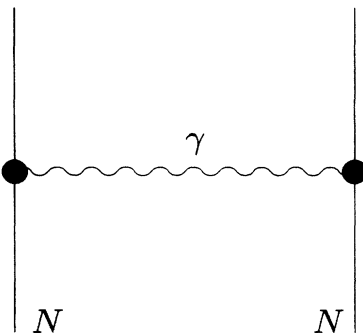


FIG. 2.  $\gamma$ -exchange between two nucleons with electromagnetic form factors.

[6], but was ultimately “thrown away” because it was assumed that the difference of the residues at the poles of the two mesons could be neglected.

The  $q^2$  variation of  $\theta(q^2)$  is an inevitable consequence of the isospin symmetry breaking and we have not used any specific models up to this stage. However, the sign and the magnitude of  $F_\rho - F_\omega$  (or  $\lambda$ ) in Eq. (2.8) depends on the QCD dynamics. In QCD, we have to start with the quark correlator instead of the hadronic correlator  $\Pi_{\mu\nu}^{\rho\omega}$ :

$$\Pi_{\mu\nu}(q^2) = i \int d^4x e^{iqx} \langle T J_\mu^\rho(x) J_\nu^\omega(0) \rangle_0, \quad (2.10)$$

where

$$J_\mu^\rho = (\bar{u}\gamma_\mu u - \bar{d}\gamma_\mu d)/2, \quad J_\mu^\omega = (\bar{u}\gamma_\mu u + \bar{d}\gamma_\mu d)/6. \quad (2.11)$$

Because the currents  $J_\mu^\rho$  and  $J_\mu^\omega$  are conserved,  $\Pi_{\mu\nu}$  has to be of transversal structure:

$$\Pi_{\mu\nu}(q^2) = (q_\mu q_\nu - g_{\mu\nu} q^2) \Pi(q^2). \quad (2.12)$$

The vector currents  $J_\mu^\rho$  and  $J_\mu^\omega$  couple to  $\rho$  and  $\omega$  as well as to the higher resonances ( $\rho', \omega', \dots$ ) and the continuum. Thus the imaginary part of  $\Pi_{\mu\nu}$  is written as the sum of all the mixed hadron correlators

$$\text{Im}\Pi_{\mu\nu}(s) = A_0 \text{Im}\Pi_{\mu\nu}^{\rho\omega}(s) + A_1 \text{Im}\Pi_{\mu\nu}^{\rho'\omega'}(s) + \dots, \quad (2.13)$$

where  $A_n$  ( $n = 0, 1, 2, \dots$ ) denotes the overlap of the quark current with the physical hadrons. For example,

$$A_0 = \frac{m_\rho^2 m_\omega^2}{g_\rho g_\omega}, \quad (2.14)$$

where  $g_{\rho,\omega}$  is defined by  $\langle 0 | J_{\mu}^{\rho,\omega} | \rho(\omega) \rangle = (m_{\rho,\omega}^2 / g_{\rho,\omega}) \epsilon_{\mu}$  with  $g_{\omega} \simeq 3g_{\rho}$  as given by flavor SU(3) and  $g_{\rho}^2/4\pi \simeq 2.4$ .

By using the dispersion relation for  $\Pi(q^2)$  and the operator-product expansion (OPE) for  $\text{Re}\Pi(q^2)$  at  $q^2 \rightarrow -\infty$ , one can extract the resonance parameters such as the mixing matrices for  $\rho$ - $\omega$  and for higher resonances on the rhs of Eq. (2.10). The first attempt at such an analysis was made by Shifman, Vainshtein, and Zakharov [16]. However, one of the mixing parameters  $\beta$ , which is related to  $\lambda$  as  $\lambda = \beta + 1$ , was not determined well because of the poor  $e^+e^-$  data available at that time and of the large uncertainty of the current quark masses. In the next section, armed with the updated information of these parameters [Eqs. (2.2) and (2.3)], we will determine the crucial quantity  $\beta$  within the framework of the QCD sum rules. The combined use of the finite energy sum rule and the Borel sum rule is a key ingredient there. From the analysis, we find that  $\lambda$  is indeed positive and, including all uncertainties in the parameters, is found to lie in an interval:

$$\lambda = \beta + 1 \in [1.43, 1.85] . \quad (2.15)$$

$\beta$  is close to, but generally larger than the value assumed in Ref. [16], 0.5. It follows that  $\theta(q^2)$  has significant  $q^2$  variation in the spacelike region; indeed, it vanishes at

$$q^2 = m^2 \frac{\lambda - 1}{\lambda} . \quad (2.16)$$

Thus the nuclear force is significantly affected by the  $q^2$  variation of  $\theta(q^2)$ . As an example we consider the leading term of the class III charge-symmetry-breaking nuclear force [17] in coordinate space. In the static limit, the radial dependence of the central  $N$ - $N$  potential from  $\rho$ - $\omega$  mixing is obtained by the Fourier transform of Eq. (2.1):

$$V_{NN}^{\rho\omega}(r) = -\frac{g_{\rho N} g_{\omega N}}{4\pi} \frac{\theta(m^2)}{2m} \left( 1 - \frac{2\lambda}{mr} \right) e^{-mr} , \quad (2.17)$$

where only the vector coupling of the nucleon to the vector mesons is taken into account. (We do not include a form factor for the coupling constants  $g_{\rho(\omega)N}$ , because we are interested in the longer range part of  $V_{NN}^{\rho\omega}$ .) When  $\lambda = 0$ , Eq. (2.17) reduces to the leading, i.e., the exponential term of the class III potential,  $-\Delta V^{\rho\omega}$ , given in [17,18]. The potential is strongly attenuated by the presence of  $\lambda$  and becomes zero at

$$r = \frac{2\lambda}{m} \sim 0.9 \text{ fm} , \quad (2.18)$$

which is, roughly, the region of interest for the symmetry-breaking effect.

### III. $\rho$ - $\omega$ MIXING IN QCD SUM RULES

#### A. Operator product expansion (OPE)

For the QCD sum rule determination of the  $\rho$ - $\omega$  mixing, one should start with the current correlator [16] given in Eqs. (2.10)–(2.12). Following Ref. [16], we will analyze sum rules obtained by the OPE for  $\Pi(q^2)$ . In the OPE series, we keep power corrections up to order 6.

Furthermore, in each term we take contributions which are of  $O(m_q)$  ( $q = u$  or  $d$ ) or of  $O(\alpha)$ , and any terms  $O(m_q^2)$ ,  $O(\alpha^2)$ , and  $O(m_q\alpha)$  are neglected. We will check the validity of these assumptions later on. Therefore we are faced with the diagrams in Fig. 3, which contribute to  $\Pi(Q^2)$  ( $Q^2 = -q^2$ ) as follows [16].

(1) *Free part* [Fig. 3(a)]. The leading order term proportional to  $\ln Q^2$  vanishes, while the next term,

$$\Pi_{(1)} = \frac{3}{2\pi^2} \frac{m_d^2 - m_u^2}{12Q^2} , \quad (3.1)$$

is of  $O(m_q^2)$  and will be neglected. For the same reason, the one-gluon exchange diagram [Fig. 3(b)] is of higher order in  $m_q$ .

(2) *Irreducible 1- $\gamma$  exchange* [Fig. 3(c)]. Because of the different coupling of the  $\gamma$  to the  $u$  and  $d$  quarks, the one- $\gamma$  exchange in Fig. 3(c) contributes as

$$\Pi_{(2)} = -\frac{\alpha}{16\pi^3} \frac{1}{12} \ln Q^2 . \quad (3.2)$$

(3) *Reducible 1- $\gamma$  exchange* [Fig. 3(d)]. As has been proposed in Ref. [16], it is convenient to separate the reducible  $\gamma$  exchange diagram from the whole analysis from the very beginning. This can be done by neglecting Fig. 3(d) in the OPE side and subtracting the  $\rho \rightarrow \gamma \rightarrow \omega$  contribution (2.3) from the phenomenological side.

(4) *Gluon condensate*  $\alpha_s \langle G^2 \rangle_0$  [Fig. 3(e)]: It vanishes for the same reason as (1).

(5) *Quark condensate*  $m_q \langle \bar{q}q \rangle_0$  [Fig. 3(f)]:

$$\Pi_{(5)} = \frac{2}{12Q^4} [m_u \langle \bar{u}u \rangle_0 - m_d \langle \bar{d}d \rangle_0] . \quad (3.3)$$

(6) *Mixed condensate* [Fig. 3(g)]. As has been shown in Refs. [16,21], even in case of only one quark flavor, these condensates contribute at least in  $O(m_q^2)$  to the vector current and are therefore not present in our analysis.

(7) *Four-quark condensate* [Figs. 3(h)–(k)]. There are contributions from gluon as well as  $\gamma$  exchanges. Typical diagrams are shown in Figs. 3(h)–(k).

(a) Fig. 3(h):

$$\Pi_{(\tau a)}(Q^2) = -\frac{2\pi\alpha_s}{12Q^6} \langle (\bar{u}\gamma_{\alpha}\gamma_5\lambda^a u)^2 - (\bar{d}\gamma_{\alpha}\gamma_5\lambda^a d)^2 \rangle_0 . \quad (3.4)$$

(b) Fig. 3(i):

$$\Pi_{(\tau b)}(Q^2) = -\frac{4\pi\alpha_s}{9 \times 12Q^6} \langle (\bar{u}\gamma_{\alpha}\lambda^a u)^2 - (\bar{d}\gamma_{\alpha}\lambda^a d)^2 \rangle_0 . \quad (3.5)$$

(c) Fig. 3(j):

$$\Pi_{(\tau c)}(Q^2) = -\frac{8\pi\alpha}{12Q^6} \langle \frac{4}{9} (\bar{u}\gamma_{\alpha}\gamma_5 u)^2 - \frac{1}{9} (\bar{d}\gamma_{\alpha}\gamma_5 d)^2 \rangle_0 . \quad (3.6)$$

(d) Fig. 3(k):

$$\Pi_{(\tau d)}(Q^2) = -\frac{16\pi\alpha}{9 \times 12Q^6} \langle \frac{4}{9} (\bar{u}\gamma_{\alpha} u)^2 - \frac{1}{9} (\bar{d}\gamma_{\alpha} d)^2 \rangle_0 . \quad (3.7)$$

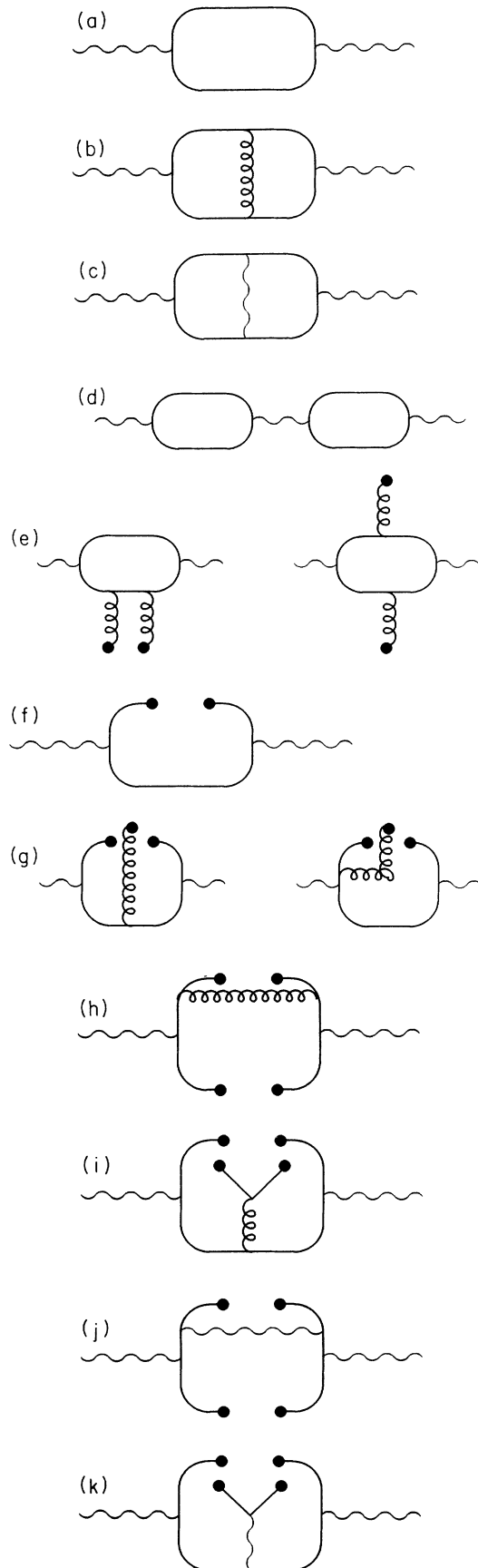


FIG. 3. Diagrams in the OPE.

### B. Symmetry-breaking parameters and vacuum condensates

There are essentially two quantities which control the isospin symmetry breaking in OPE:  $m_d/m_u$  and  $\langle \bar{d}d \rangle_0 / \langle \bar{u}u \rangle_0$ . Although they are related in principle in QCD, they appear as independent parameters in the QCD sum rules. As we will see below, the dimension four operator in the OPE is controlled by the quark mass ratio while the dimension six operator depends on the ratio of the condensates. Because the dimension four operator is the dominant term in the OPE, the  $\rho$ - $\omega$  mixing is essentially determined by the quark mass ratio and depends weakly on the ratio of the condensates.

The quark mass ratio is determined by the analysis of the mass splitting of mesons and barons using the chiral perturbation theory ([20] and references therein):

$$\frac{m_d - m_u}{m_d + m_u} = 0.28 \pm 0.03. \quad (3.8)$$

The isospin breaking of the quark condensate has been analyzed by several methods; the chiral perturbation theory [22], the QCD sum rules for scalar and pseudoscalar mesons [23–25], effective models of QCD incorporating the dynamical breaking of chiral symmetry [26,27], and the QCD sum rules for baryons [28]:

$$\gamma = \frac{\langle \bar{d}d \rangle_0}{\langle \bar{u}u \rangle_0} - 1 = \begin{cases} -(6-10) \times 10^{-3} & [22], \\ -(10 \pm 3) \times 10^{-3} & [23], \\ -(7-9) \times 10^{-3} & [26,27], \\ -(2 \pm 1) \times 10^{-3} & [28]. \end{cases} \quad (3.9)$$

Here we have assumed  $\langle \bar{s}s \rangle_0 / \langle \bar{u}u \rangle_0 - 1 = -(15-30)\%$  to get the first number in the above. The last number is obtained solely by using the baryon mass splittings in the QCD sum rule and is quite different from the other determinations.

Besides the symmetry-breaking parameters, we need to fix the value of the four-quark condensate. The vacuum saturation hypothesis gives a rough estimate of its magnitude; it gives a satisfactory description of the  $\rho$ -meson properties [14]. However, there are recent arguments which favor a value larger by a factor 2 or more than that adopted in [14] (see, e.g., [15,29] and the references therein). Since this condensate is not determined well in the sum rule, we will take the following two typical numbers and carry out the Borel analysis using them:

$$\alpha_s \langle \bar{q}q \rangle_0^2 = \begin{cases} 1.81 \times 10^{-4} \text{ GeV}^6 & \text{vacuum saturation [14]} \\ 3.81 \times 10^{-4} \text{ GeV}^6 & [29]. \end{cases} \quad (3.10)$$

The definition of  $\gamma$  in Eq. (3.9) and the vacuum saturation hypothesis allow us to rewrite the isospin breaking in the four-quark condensate as

$$\langle \bar{u}u \rangle_0^2 - \langle \bar{d}d \rangle_0^2 = -2\gamma \langle \bar{q}q \rangle_0^2, \quad (3.11)$$

$$\alpha \langle \bar{u}u \rangle_0^2 = \alpha \langle \bar{d}d \rangle_0^2 = \alpha \langle \bar{q}q \rangle_0^2. \quad (3.12)$$

Using the above symmetry-breaking parameters and the vacuum condensates together with the Gell-Mann–Oakes–Renner relation [30]

$$(m_u + m_d) \langle \bar{u}u + \bar{d}d \rangle_0 = -2f_\pi^2 m_\pi^2, \quad (3.13)$$

Eq. (3.3) and the sum of (3.4)–(3.7) are written as

TABLE I. The sets I-IV of input parameters for the OPE.

	$10^4 \xi$	$\frac{m_d - m_u}{m_d + m_u}$	$10^3 \gamma$	$\alpha_s \langle \bar{q}q \rangle_0^2 (10^4 \text{ GeV}^6)$
Set I	$11.3 \pm 1.3$	$0.28 \pm 0.03$	$-9.0 \pm 3.0$	1.81
Set II	$11.3 \pm 1.3$	$0.28 \pm 0.03$	$-9.0 \pm 3.0$	3.81
Set III	$11.3 \pm 1.3$	$0.28 \pm 0.03$	$-2.0 \pm 1.0$	1.81
Set IV	$11.3 \pm 1.3$	$0.28 \pm 0.03$	$-2.0 \pm 1.0$	3.81

$$\Pi_{(5)}(Q^2) = \frac{1}{12Q^4} \frac{m_d - m_u}{m_d + m_u} 2f_\pi^2 m_\pi^2 \left[ 1 + \frac{m_d + m_u}{m_d - m_u} \frac{\gamma}{2 + \gamma} \right], \quad (3.14)$$

and

$$\Pi_{(7)}(Q^2) = -\frac{224}{81} \frac{2}{12Q^6} \pi [\alpha_s \langle \bar{q}q \rangle_0^2] \left[ -\gamma + \frac{\alpha}{8\alpha_s(\mu^2)} \right]. \quad (3.15)$$

Summing up all contributions, we obtain

$$12\Pi(Q^2) = -c_0 \ln Q^2 + \frac{c_1}{Q^2} + \frac{c_2}{Q^4} + 2\frac{c_3}{Q^6}, \quad (3.16)$$

with

$$c_0 = \frac{\alpha}{16\pi^3}, \quad (3.17)$$

$$c_1 = \frac{3}{2\pi^2} (m_d^2 - m_u^2) \sim 0, \quad (3.18)$$

$$c_2 = \frac{m_d - m_u}{m_d + m_u} 2f_\pi^2 m_\pi^2 \left[ 1 + \frac{m_d + m_u}{m_d - m_u} \frac{\gamma}{2 + \gamma} \right], \quad (3.19)$$

$$c_3 = -\frac{224}{81} \pi [\alpha_s \langle \bar{q}q \rangle_0^2] \left[ -\gamma + \frac{\alpha}{8\alpha_s(\mu^2)} \right]. \quad (3.20)$$

For the renormalization point  $\mu^2$ , we take a typical scale of the Borel mass 1 GeV<sup>2</sup>, so that

$$\alpha_s = \alpha_s(1 \text{ GeV}^2) \sim 0.5. \quad (3.21)$$

It is obvious from Eqs. (3.19) and (3.20) that the  $m_d/m_u$  controls the magnitude of the dimension four matrix element and  $\langle \bar{d}d \rangle_0 / \langle \bar{u}u \rangle_0$  controls the dimension six matrix element.

The aim of our sum rule analysis is to determine the parameter  $\beta$  (or  $\lambda$ ); we will use the experimental  $\rho$ - $\omega$  mixing at  $q^2 = m_\omega^2$  as an input. For later use, let us define here the dimensionless mixing of hadronic origin as

$$\xi = \frac{-12 \theta(m^2) - \theta_{\rho \rightarrow \gamma \rightarrow \omega}}{g_\rho g_\omega m^2} = (11.3 \pm 1.3) \times 10^{-4}. \quad (3.22)$$

TABLE II. The OPE coefficients  $c_i$  ( $i = 0, \dots, 3$ ) in units of  $m^2 \cdot 10^{-4}$  calculated with the parameter sets I-IV from Table I.

	$c_0$	$c_1$	$c_2$	$c_3$
Set I	0.147	0	$2.66 \pm 0.30$	$-0.83 \pm 0.23$
Set II	0.147	0	$2.66 \pm 0.30$	$-1.75 \pm 0.48$
Set III	0.147	0	$2.70 \pm 0.30$	$-0.29 \pm 0.08$
Set IV	0.147	0	$2.70 \pm 0.30$	$-0.61 \pm 0.17$

To take into account the large uncertainties of  $\gamma$  and  $\alpha_s \langle \bar{q}q \rangle_0^2$ , we perform our analysis for the four different sets of input parameters specified in Table I with the corresponding OPE coefficients  $c_i$  ( $i = 0, \dots, 3$ ) shown in Table II. Borel stability analyses will be made for these four different sets in Sec. III E.

### C. Spectral function and sum rule

The general expression for the spectral function, i.e., the imaginary part of  $\Pi_{\mu\nu}(q^2)$  is given in Eq. (2.13). As has been pointed out in Refs. [16,15], it is absolutely necessary to keep at least one higher resonance ( $\rho'$ ,  $\omega'$ ) in (2.13) in order to obtain stability in the QCD sum rule. We will treat the related mass  $m'^2 = \frac{1}{2}(m_{\rho'}^2 + m_{\omega'}^2)$  as well as the corresponding coupling constants  $g_{\rho'}$  and  $g_{\omega'}$  as effective parameters to be determined from the Borel stability analysis. Furthermore, in order to account for the electromagnetic logarithm in Eq. (3.2) in the space-like region, we have to introduce a continuum threshold  $s_0$ . The corresponding part in the spectral function is “suppressed” by the electromagnetic coupling  $\alpha$  and indeed it will turn out that the influence of this term on the sum rule analysis is very small. Assuming sharp resonances for  $\rho$ ,  $\omega$ ,  $\rho'$ , and  $\omega'$  as well as a step function for the continuum one can write, analogous to Eq. (2.6),

$$12\text{Im}\Pi(s) = \pi f_\rho \delta(s - m_\rho^2) - \pi f_\omega \delta(s - m_\omega^2) \\ + \pi f_{\rho'} \delta(s - m_{\rho'}^2) - \pi f_{\omega'} \delta(s - m_{\omega'}^2) \\ + \frac{\alpha}{16\pi^2} \theta(s - s_0). \quad (3.23)$$

The general form of the Borel sum rule reads [16]:

$$\frac{1}{\pi M^2} \int_0^\infty ds e^{-s/M^2} \text{Im}\Pi(s) = \tilde{\Pi}_B(M^2), \quad (3.24)$$

where the Borel transform  $\tilde{\Pi}_B(M^2)$  is defined by

$$\tilde{\Pi}_B(M^2) = \lim_{\substack{Q^2, n \rightarrow \infty \\ M^2 = Q^2/n \text{ fixed}}} \frac{1}{(n-1)!} Q^{2n} \left( \frac{d^2}{dQ^2} \right)^n \Pi(Q^2). \quad (3.25)$$

Let us define the following parameters:

$$\begin{aligned}\xi &= \frac{\delta m^2 f_\rho + f_\omega}{m^4} \frac{1}{2}, \\ \xi' &= \frac{\delta m'^2 f_{\rho'} + f_{\omega'}}{m'^4} \frac{1}{2},\end{aligned}\quad (3.26)$$

$$\begin{aligned}\beta &= -(f_\rho - f_\omega)m^2 \left[ \frac{\delta m^2 f_\rho + f_\omega}{2} \right]^{-1}, \\ \beta' &= -(f_{\rho'} - f_{\omega'})m'^2 \left[ \frac{\delta m'^2 f_{\rho'} + f_{\omega'}}{2} \right]^{-1}.\end{aligned}\quad (3.27)$$

$\xi$  and  $\xi'$  are directly related to the on-mass-shell mixing in the  $\rho$ - $\omega$  and  $\rho'$ - $\omega'$  channels, respectively.  $\beta$  and  $\beta'$  are related to the isospin symmetry breaking at the resonance poles and control the  $q^2$  dependence of the  $\rho$ - $\omega$  and  $\rho'$ - $\omega'$  mixing. The relation between  $\beta$  and  $\lambda$  defined in Sec. II is easily obtained by comparing (2.13), (2.14), (2.6), with (2.12) and (3.23), which gives

$$f_{\rho,\omega} = \frac{A_0}{m_{\rho,\omega}^2} F_{\rho,\omega} \quad (3.28)$$

and therefore

$$\lambda = \beta + 1. \quad (3.29)$$

By using the above definitions, one obtains from Eq. (3.16) up to  $O(\delta m^2)$  and  $O(\delta m'^2)$  the Borel sum rule (BSR):

$$\begin{aligned}\xi \frac{m^2}{M^2} \left( \frac{m^2}{M^2} - \beta \right) e^{-m^2/M^2} + \xi' \frac{m'^2}{M^2} \left( \frac{m'^2}{M^2} - \beta' \right) e^{-m'^2/M^2} + \frac{\alpha}{16\pi^3} e^{-s_0/M^2} \\ = c_0 + c_1 \left( \frac{m^2}{M^2} \right) + c_2 \left( \frac{m^2}{M^2} \right)^2 + c_3 \left( \frac{m^2}{M^2} \right)^3,\end{aligned}\quad (3.30)$$

where  $c_0$ - $c_3$  are in units of  $10^{-4}$ .

Starting from this expression, one can carry out the Borel analysis (stability analysis with respect to  $M^2$ ) or analysis of the finite energy sum rule (expansion in  $1/M^2$  on both sides). Let us summarize our strategy before entering into the details. On the right-hand side of Eq. (3.30), we have seven resonance parameters:  $\beta$ ,  $\beta'$ ,  $\xi$ ,  $\xi'$ ,  $m$ ,  $m'$ , and  $s_0$ . Among them,  $m$  is the average mass of  $\rho$  and  $\omega$ , and  $\xi$  is directly related to the measured  $\rho$ - $\omega$  mixing, so they are known inputs.  $m'$  should be chosen to be a number close to  $m_{\rho'} = 1390$  MeV or  $m_{\omega'} = 1450$  MeV; thus it is not arbitrary. The sum rule depends on  $s_0$  very weakly because of the suppression by  $\alpha$ ; thus the choice of  $s_0$  does not materially affect the result. Hence we are left with essentially three unknown parameters  $\beta$ ,  $\beta'$ , and  $\xi'$  to be determined by the sum rule.

In the finite energy sum rule (FESR), by expanding Eq. (3.30) in powers of  $1/M^2$ , we get three independent equations. They are enough to solve for the three unknowns. One can also change  $m'$  and  $s_0$  slightly to check the sensitivity of the result to that change. One of the problems of the FESR when compared to the Borel sum rule is that it is generally sensitive to the parameters of the higher resonances. Therefore, after getting a rough idea for the magnitude and sign of the three unknowns, we will move on to the Borel sum rule.

By taking a derivative of Eq. (3.30) with respect to  $M^2$ , one generates another independent sum rule. To carry out the stability analysis for each unknown parameter ( $\beta$ ,  $\beta'$ , and  $\xi'$ ), we need one more constraint, and we take a first sum rule of the FESR to supply this constraint. The first sum rule is known to be a local duality relation and is least sensitive to the higher resonances. By this procedure, we can draw independent Borel curves

for each unknown and carry out the stability analysis by varying  $m'$  and  $s_0$ , i.e.,  $m'$  and  $s_0$  are chosen such that  $\beta$ ,  $\beta'$ , and  $\xi'$  are least sensitive to the variation of the Borel mass  $M^2$ . In this way, we can completely determine the resonance parameters within the QCD sum rules. Our procedure is different from the original SVZ analysis [16] where  $\beta$  was assumed to be 1/2 as an input and also poor experimental data of  $\xi$  was used.

#### D. Finite energy sum rule (FESR)

The FESR can be formally obtained by expanding the BSR Eq. (3.30) in powers of  $\frac{1}{M^2}$  and comparing the coefficients of each power on both sides. In doing so one obtains three FESR's:

$$-\beta\xi - \beta'\xi' \frac{m'^2}{m^2} - c_0 \frac{s_0}{m^2} = c_1, \quad (3.31)$$

$$\xi + \xi\beta + \xi' \frac{m'^4}{m^4} + \xi'\beta' \frac{m'^4}{m^4} + \frac{1}{2}c_0 \left( \frac{s_0}{m^2} \right)^2 = c_2, \quad (3.32)$$

$$-\xi - \frac{1}{2}\xi\beta - \xi' \frac{m'^6}{m^6} - \frac{1}{2}\xi'\beta' \frac{m'^6}{m^6} - \frac{1}{6}c_0 \left( \frac{s_0}{m^2} \right)^3 = c_3. \quad (3.33)$$

Using various values for  $m'^2$  and  $s_0$  as input parameters we can therefore solve Eqs. (3.31)–(3.33) which gives us the three unknown parameters  $\beta$ ,  $\xi'$ , and  $\beta'$ . Table III shows their values for the OPE set I. As we can see, the result is sensitive to the choice of the resonance mass  $m'^2$ , whereas the influence of the electromagnetically sup-

TABLE III.  $\beta$ ,  $\xi'$ , and  $\beta'$  from the FESR for different values of  $m'^2$  and  $s_0$  (parameter set I).

$(m'^2, s_0)$ (GeV <sup>2</sup> )	$\beta$	$\xi'$	$\beta'$
(1.4, 2.0)	0.91	1.03	-4.41
(1.6, 2.0)	0.75	0.87	-3.79
(1.8, 2.0)	0.64	0.74	-3.44
(2.0, 2.0)	0.55	0.62	-3.20
(1.8, 1.4)	0.64	0.73	-3.38
(1.8, 2.0)	0.64	0.74	-3.44
(1.8, 2.4)	0.64	0.73	-3.52

pressed threshold  $s_0$  is small.

It is important to notice that  $\beta\xi$  and  $\beta'\xi'$  have to be opposite in sign due to the first FESR (3.31) or equivalently the local duality relation,

$$\int_0^\infty ds \text{Im}\Pi(s) = O(\alpha) \approx 0, \quad (3.34)$$

$$\beta(M^2) = \frac{1}{\xi} \frac{Z_2(M^2) + Z_1(M^2) \left(1 - \frac{m'^2}{m^2}\right)}{W_1(M^2) \left(\frac{m'^2}{m^2} - 1\right) - W_2(M^2)}, \quad (3.35)$$

$$\xi'(M^2) = \left(\frac{M^2}{m^2}\right)^2 e^{m'^2/M^2} [\beta(M^2)\xi W_1(M^2) + Z_1(M^2)], \quad (3.36)$$

$$\beta'(M^2) = \frac{1}{\xi'(M^2)} \left[-\beta(M^2)\xi \frac{m^2}{m'^2} - c_0 \frac{s_0}{m'^2} - c_1 \frac{m^2}{m'^2}\right], \quad (3.37)$$

with

$$\begin{aligned} Z_1(M^2) &= c_0 \left[1 - e^{-s_0/M^2} - \frac{s_0}{M^2} e^{-m'^2/M^2}\right] + c_1 \frac{m^2}{M^2} \left(1 - e^{-m'^2/M^2}\right) - \xi \left(\frac{m^2}{M^2}\right)^2 e^{-m^2/M^2} + c_2 \left(\frac{m^2}{M^2}\right)^2 \\ &\quad + c_3 \left(\frac{m^2}{M^2}\right)^3, \\ W_1(M^2) &= \frac{m^2}{M^2} \left(e^{-m^2/M^2} - e^{-m'^2/M^2}\right), \\ Z_2(M^2) &= \frac{1}{M^4} \left[-\frac{\partial}{\partial(1/M^2)} [M^2 Z_1(M^2)]\right], \\ W_2(M^2) &= \frac{1}{M^4} \left[-\frac{\partial}{\partial(1/M^2)} [M^2 W_1(M^2)]\right]. \end{aligned} \quad (3.38)$$

The general procedure for determining  $m'^2$  and  $s_0$  is now the following: For each of the parameter sets I–IV from Table I we first take the corresponding central value (i.e., without error bars) of the OPE coefficients  $c_i$  ( $i = 1, \dots, 3$ ) from Table II and calculate the Borel curves  $\beta(M^2)$ ,  $\xi'(M^2)$ , and  $\beta'(M^2)$  due to Eqs. (3.36), (3.37), and (3.37), respectively, for various values of  $m'^2$  and  $s_0$ . The final result is the one with the least dependence on  $M^2$  within the Borel window  $M^2 \geq M_{\min}^2$  with  $M_{\min}^2$  determined above. The results for  $\beta$  and  $\xi'$  using parameter set I are shown in Figs. 4 and 5, respectively. One recognizes a wide stable region, which even can be

This is the reason why one should keep the resonance explicitly [16], otherwise the term  $\beta\xi$  cannot be canceled.

### E. Borel analysis

Finally we perform the Borel stability analysis of (3.30). Again we take for  $\xi$  the experimental input (3.22).  $m'^2$  and  $s_0$  are used as variable parameters which are fixed in order to obtain maximal stability of the Borel curves. In order to choose a stability window for  $M^2$ , we demand that, for each parameter set (I–IV), the contribution of the sixth order power correction in the OPE is less than 25% of the fourth order one. This gives a lower limit  $M_{\min}^2$  for the Borel mass  $M^2$ .

As we mentioned before, we adopt the first sum rule of the FESR (3.31) or equivalently the local duality relation (3.34) as an additional constraint. Also, we generate another sum rule from (3.30) by operating with  $\left[\frac{1}{M^4} \left(-\frac{\partial}{\partial(1/M^2)}\right) M^2\right]$  on both sides. In doing so one can uniquely calculate the three unknown parameters  $\beta$ ,  $\xi'$ , and  $\beta'$  as function of  $M^2$ :

extended up to  $M^2 \approx 10$  GeV<sup>2</sup>. The maximal stability occurs for  $m'^2 = 1.6$  GeV<sup>2</sup>, where  $s_0$  can be increased up to about 2.4 GeV<sup>2</sup> without any significant change. This insensitivity of the result to the variation of the continuum threshold are found for all other parameter sets as well and reflects the fact that the dependence on  $s_0$  is suppressed by the electromagnetic coupling  $\alpha$ . With  $m'^2$  and  $s_0$  obtained in this way, we now consider the change in the Borel curves for  $\beta$ ,  $\xi'$ , and  $\beta'$  for the upper and lower limits of  $c_i$  from Table II and extract from this the upper and lower limits for  $\beta$ ,  $\xi'$ , and  $\beta'$ . For  $\beta$  (set I) the limits are shown in Fig. 6. The final values are given in Table



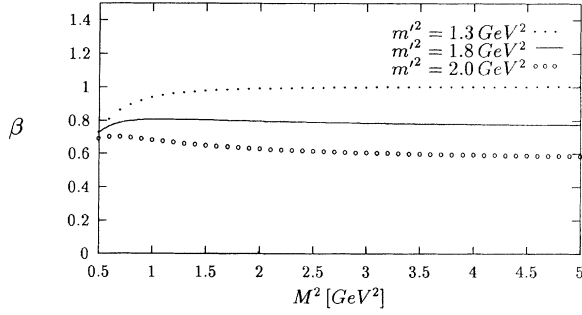


FIG. 4. Borel curve for  $\beta$  with three different values of  $(m'^2, s_0)$  (parameter set I.)

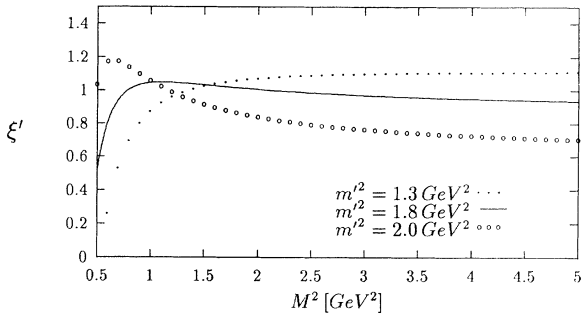


FIG. 5. Borel curve for  $\xi'$  with three different values of  $(m'^2, s_0)$  (parameter set I.)

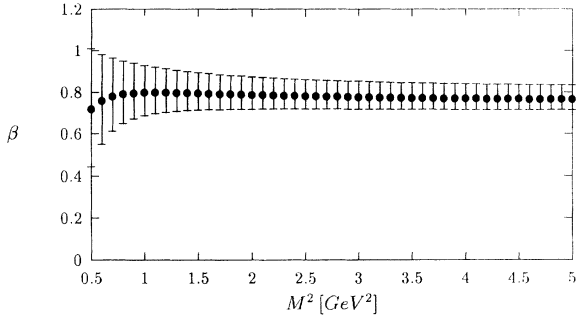


FIG. 6. Variation of  $\beta(M^2)$  due to the errorbars in Table I and Table II where  $m'^2 = 1.6 \text{ GeV}^2$  and  $s_0 = 1.8 \text{ GeV}^2$  are fixed and taken from Fig. 4 as the values with maximal Borel stability in the window  $M^2 \geq M_{\min}^2 = 1.0 \text{ GeV}^2$ .

TABLE IV. The final values of  $\beta$ ,  $\xi'$ , and  $\beta'$  as well as the resonance mass  $m'^2$  for the four different parameter sets of Table I extracted from the Borel stability analysis.

	$\beta$	$\xi'$	$\beta'$	$m'^2$
Set I	$0.78 \pm 0.07$	$0.98 \pm 0.17$	$-3.52 \pm 0.30$	1.6
Set II	$0.65 \pm 0.13$	$0.85 \pm 0.46$	$-2.71 \pm 0.60$	2.0
Set III	$0.47 \pm 0.04$	$0.56 \pm 0.07$	$-2.61 \pm 0.15$	2.4
Set IV	$0.62 \pm 0.06$	$0.76 \pm 0.11$	$-3.06 \pm 0.23$	1.9

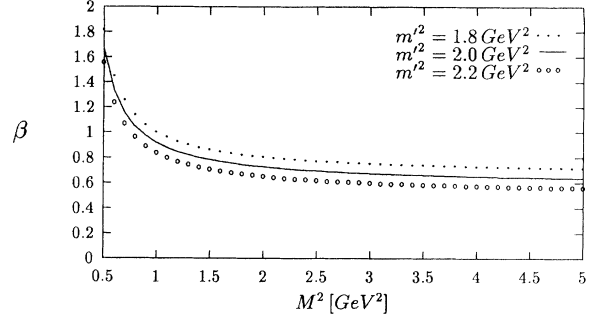


FIG. 7. Borel curve for  $\beta$  with three different values of  $(m'^2, s_0)$  (parameter set II.)

IV. It turns out that the variation of  $\beta$ ,  $\xi'$ , and  $\beta'$  is completely determined by the variation of the coefficient  $c_2$ , which itself is based on the uncertainty of the quark mass difference  $(m_d - m_u)/(m_d + m_u) = 0.28 \pm 0.03$ . The uncertainty of  $\gamma$ , which creeps into the coefficient  $c_3$  of the dimension six condensate can be neglected. It should be noted that a full readjustment of  $m'^2$  and  $s_0$  for the upper and lower limits of the  $c_i$ 's from Table II which are obtained by performing a new stability analysis for each case would result in much bigger error bars for  $\beta$ ,  $\xi'$ , and  $\beta'$ .

Similar considerations hold for parameter sets III and IV. In the case of set II we find that the Borel curves are rather unstable in the window  $M^2 \geq M_{\min}^2 = 1.5 \text{ GeV}^2$  (Figs. 7 and 8), especially the one for  $\xi'$ , and therefore this uncertainty, which is bigger than the variation due to the  $c_i$ 's, has to be included in the corresponding error bars of Table IV.

Finally we have convinced ourselves that in none of these cases does the result change noticeably if one either switches off the electromagnetic interaction completely, i.e., puts  $\alpha$  equal to zero, or includes the  $O(m_q^2)$  diagram [Fig. 3(a)] with the corresponding coefficient  $c_1$  in the Borel analysis; this analysis justifies the neglect of these terms in higher orders.

We also want to stress that the value of  $\beta$  obtained by this method differs significantly from that used in Ref. [16],  $\beta = 0.5$ , which was based on an SU(3) symmetry argument and served as input parameter. Also the individual signs of  $\xi'$  and  $\beta'$  come out different than in

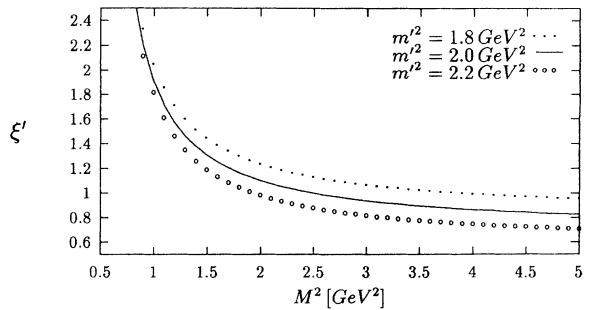


FIG. 8. Borel curve for  $\xi'$  with three different values of  $(m'^2, s_0)$  (parameter set II.)

[16], which arises from the fact that, in addition to  $\beta$ , a different experimental value of  $\xi$  was used there.

#### IV. THE OFF-SHELL $\rho$ - $\omega$ MIXING AND THE $N$ - $N$ POTENTIAL

In the previous section, we have determined the parameter  $\beta$  ( $=\lambda - 1$ ) which controls the  $q^2$  dependence of the  $\rho$ - $\omega$  mixing parameter  $\theta(q^2)$ . The result summarized in Table IV together with the relation between  $\lambda$  and  $\theta(q^2)$  [Eq. (2.9)] immediately leads to Fig. 9. The region inside the shaded band of Fig. 9 is favored by our QCD sum rule analyses.

An important observation is that  $\lambda$  is always greater than 1 as long as  $\beta$  is positive. This feature leads to the conclusion that  $\theta(q^2)$  already changes sign for *positive*  $q^2$  and is always negative for  $q^2 < 0$ , as can be seen in Fig. 9. Although the considerable variation of  $\theta(q^2)$  obtained here is qualitatively similar to previous results based on different models, our  $\theta(q^2)$  has a stronger  $q^2$  dependence than that of others.

In the quark-loop model ( $\rho \rightarrow q\bar{q} \rightarrow \omega$ ) with momentum cutoff [8],  $\theta(q^2)$  changes sign at a spacelike momentum ( $q^2 \sim -m_\rho^2/2$ ), therefore the variation of  $\theta(q^2)$  is more moderate than ours. The nucleon-loop model ( $\rho \rightarrow N\bar{N} \rightarrow \omega$ ) with dimensional regularization [9] predicts a sign change of  $\theta(q^2)$  at  $q^2 = 0$ , which still corresponds to a more moderate variation than our result.

One should notice here that there is a crucial assumption with no theoretical justification in both quark-loop and nucleon-loop models: the effect of the isospin breaking other than the QED effect is solely attributed to the mass difference between  $u$  and  $d$  constituent quarks (in the quark-loop model) or to the mass difference between the proton and the neutron (in the nucleon-loop model). There is no *a priori* reason, however, to neglect the isospin breaking in the coupling constants of the vector mesons with the constituent quarks or the nucleons, which generates an extra effect to the  $\rho$ - $\omega$  mixing of  $O(m_d - m_u)$ ; nor is there justification for neglecting nuclear resonances, e.g.,  $\Delta$ ,  $N^*$ . Thus it is fair to say that Refs. [8,9] take into account only a part of the total contribution due to the current-quark mass difference. We do not suffer from this deficiency, since all the isospin

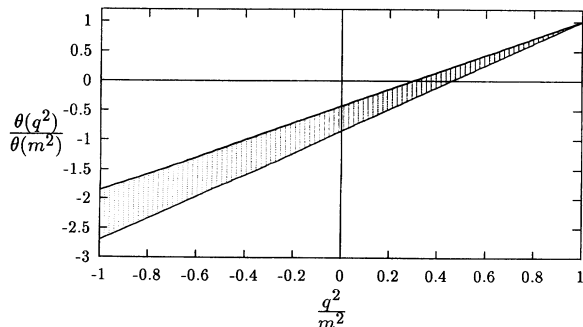


FIG. 9. The off-shell  $\rho$ - $\omega$  mixing angle  $\theta(q^2)$  with  $\beta = 0.78$ .

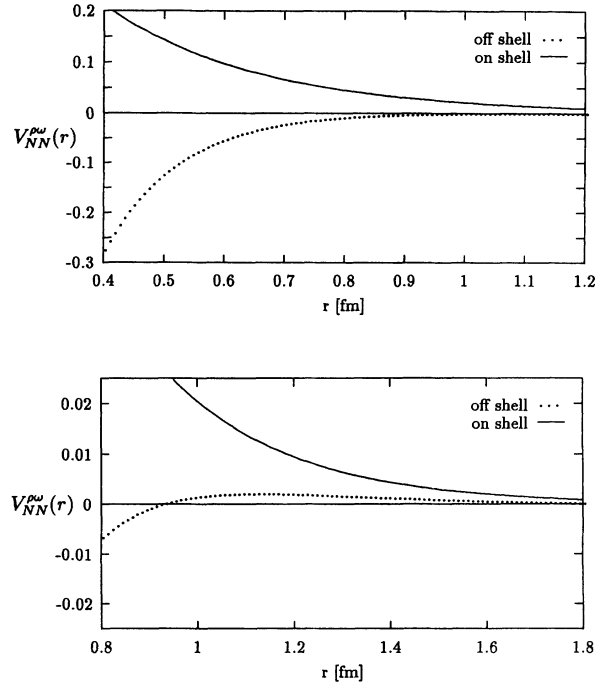


FIG. 10. The  $N$ - $N$  potential resulting from the  $\rho$ - $\omega$  mixing  $V_{NN}^{\rho\omega}(r)$  (in arbitrary units) calculated with  $\lambda = 1.78$  (dotted line) [which is the result for parameter set I (cf. Table I)] in comparison with using the *on-shell* value for  $\theta$  (corresponding to  $\lambda = 0$ ) [17] (full line). The second figure magnifies the relevant region of  $r$ , where the sign change of the off-shell curve takes place.

breaking effects are automatically taken into account in the OPE of the current correlator.

Let us also comment on the unsubtracted dispersion relation (2.5) for  $\Pi^{\rho\omega}(q^2)$  which we have used to extract  $\theta(q^2)$  from  $\text{Im}\Pi^{\rho\omega}(q^2)$ . As can be seen from the OPE in Sec. III, the function  $\Pi(q^2)$  behaves like  $1/q^2$  as  $q^2 \rightarrow -\infty$  if we switch off the small QED effect. Therefore the dispersion integral (2.5) is convergent and there is no need of a subtraction to extract  $\text{Re}\Pi^{\rho\omega}(q^2)$  for the entire  $q^2$  region from the spectral function obtained from the QCD sum rule. This is the reason why we could *predict* the  $q^2$  dependence of the mixing. If a subtraction were necessary, then extra experimental information would have been required to fix the subtraction constant.<sup>1</sup>

The  $q^2$  variation of  $\theta(q^2)$  is of primary interest for the isospin breaking  $N$ - $N$  interaction shown in Fig. 1. As an example let us consider the leading contribution to the class III  $N$ - $N$  potential, including the effect of  $\theta(q^2)$ , which is given by Eq. (2.17). To compare the potential  $V_{NN}^{\rho\omega}(r)$  with and without the  $q^2$  dependence, we have shown  $V_{NN}^{\rho\omega}(r)$  in Fig. 10 for  $\lambda = \beta + 1$  (the dotted line)

<sup>1</sup>When we determine the phenomenological parameters in the spectral function  $\text{Im}\Pi(s)$  of the QCD sum rule, the subtraction is irrelevant since the Borel sum rule is used.

and  $\lambda = 0$  the (the full line), where we have used  $\beta = 0.78$  from set I (cf. Table IV) as a typical example. The long range exponential potential due to the  $\rho$ - $\omega$  mixing (the first term in Eq. (2.17)) is strongly suppressed by the  $q^2$  dependence of the mixing [second term in Eq. (2.17)]. As a result, in the coordinate space the potential changes sign at  $r = 2\lambda/m = 0.9$  fm. The large difference between the solid and the dashed curves of Fig. 10 at short distances is not really relevant, since the short range part of the potential  $V_{NN}^{\rho\omega}(r)$  is screened by the strong central repulsion of the nuclear force and also is reduced by the the  $\rho$ - $N$ - $N$  and  $\omega$ - $N$ - $N$  form factors.

Of course it is clear that the  $q^2$  dependence of  $\theta$  [Eq. (2.9)] has a similar influence on the class IV nuclear potential as well.

Several remarks are in order here on the  $N$ - $N$  potential due to the isospin breaking.

(1) In the conventional application of the  $\rho$ - $\omega$  mixing to the  $N$ - $N$  potential, only the mixing of the  $\rho$ - $\omega$  propagators is taken into account, as is shown in Fig. 1. However, there is another source of isospin breaking due to the isospin-breaking  $\rho(\omega)$ - $N$ - $N$  coupling (cf. Fig. 11). The magnitude of this symmetry breaking is unknown. This effect does not contribute to the polarization difference in  $n$ - $p$  scattering, but does contribute to the Nolen-Schiffer anomaly.

(2) The QCD sum rule can give us the mixing in the  $\rho$ - $\omega$  channel and that in the  $\rho'$ - $\omega'$  channel separately. Therefore we can study the effect of  $\rho'$ - $\omega'$  mixing to the  $N$ - $N$  force. From the QCD sum rule we have extracted  $\beta' \approx -2.5, \dots, -3.5$ , so that the corresponding  $\lambda' = \beta' + 1$  is clearly negative and therefore the effect goes into the other direction, i.e., the  $\rho'$ - $\omega'$  mixing angle  $\theta'(q^2)$  increases in the spacelike region. The effect of  $\theta'(q^2)$  ( $\rho'$ - $\omega'$  mixing) to the nuclear force will appear only at short distances compared to  $\theta(q^2)$  ( $\rho$ - $\omega$  mixing). Thus it is not so relevant to the low-energy  $N$ - $N$  scattering. Since we do not have any information of the  $\rho'(\omega')$ - $N$ - $N$  coupling constants, we cannot make any quantitative estimate to the effect of  $\theta'(q^2)$  at the present stage. In the one-boson exchange approach to the nuclear force the higher resonance contributions are not taken into account explicitly.

(3) In our approach we have taken a sharp resonance for the  $\rho$  meson spectral function and therefore completely neglected the width of the  $\rho$  meson. However we believe that including the  $\rho$  meson width does not change our result significantly, because only the integral over the spectral function is important in the sum rule and furthermore the crucial quantity  $\lambda = \beta + 1 > 1$  does not depend so much on the details of the calculation of  $\beta$ .

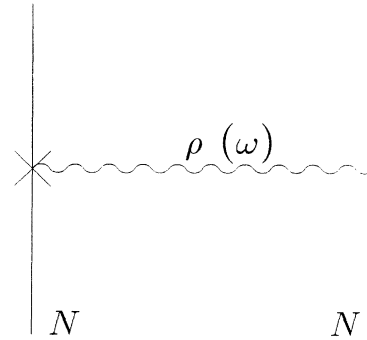


FIG. 11. Isospin breaking nuclear force due to  $\rho$  or  $\omega$  exchange with isospin breaking  $\rho(\omega)$ - $N$ - $N$  vertex.

## V. SUMMARY AND CONCLUSIONS

QCD sum rules have been shown to be a powerful technique for studying meson and baryon properties. In this paper we have used these sum rules together with the usual unsubtracted dispersion relation to study  $\rho$ - $\omega$  mixing both on- and off-mass shells. We find a rapid variation of the mixing parameter  $\theta(q^2)$  with  $q^2$ . Thus, although we fit the value of  $\theta$  at  $q^2 = m_\rho^2 \approx m_\omega^2$ , its sign has already changed at  $q^2 = 0$ . Since it is the spacelike value of  $q^2$  that plays a role in the contribution of  $\rho$ - $\omega$  mixing to the nuclear force, our results have important implications for fitting experimental results. For example, the on-shell value of the  $\rho$ - $\omega$  mixing parameter,  $\theta(m^2)$ , has been used to fit the asymmetry observed in polarized  $n$ - $p$  scattering [1-3,7]. Indeed, at  $\approx 200$  MeV, this (assumed on-mass-shell) mixing gives the dominant contribution to the observed asymmetry. Our results, like those obtained previously by other methods [8,9], thus place a large question mark on our understanding of the observed charge asymmetry. In addition  $\rho$ - $\omega$  mixing contributes to the difference of the  $p$ - $p$  and  $n$ - $n$  scattering lengths and to the energy differences of mirror nuclei. Indeed, there has been a revival of interest [13] in the contribution of  $\rho$ - $\omega$  mixing to the Nolen-Schiffer anomaly [4,5] and our result also puts some of these explanations [10] into questions.

## ACKNOWLEDGMENTS

This work has been supported in part by the Department of Energy (T.H., E.H., and T.M.) and the Alexander von Humboldt-Stiftung (Feodor-Lynen Program) (T.M.). G.K. wishes to thank the Nuclear Theory Group of the University of Washington for financial support.

- [1] G. A. Miller, B. M. K. Nefkens, and I. Šlaus, Phys. Rep. **194**, 1 (1990).
- [2] R. Abegg *et al.*, Phys. Rev. Lett. **56**, 2571 (1986); Phys. Rev. D **39**, 2464 (1989).
- [3] L. D. Knutson *et al.*, Nucl. Phys. **A508**, 185 (1990); S.E. Vigdor *et al.* Phys. Rev. C **46**, 410 (1992).
- [4] J. A. Nolen, Jr. and J. P. Schiffer, Annu. Rev. Nucl. Sci.

**19**, 471 (1969).

- [5] S. Shlomo, Rep. Prog. Phys. **41**, 957 (1978).
- [6] E. M. Henley and G. A. Miller, in *Mesons and Nuclei*, edited by M. Rho and D. H. Wilkinson (North-Holland, Amsterdam, 1979).
- [7] G. A. Miller, A. W. Thomas, and A. G. Williams, Phys. Rev. Lett. **56**, 2567 (1986); Phys. Rev. C **36**, 1956 (1987).

- [8] T. Goldman, J. A. Henderson, and A. W. Thomas, *Few Body Systems* **12**, 123 (1992).
- [9] J. Piekarewicz and A. G. Williams, *Phys. Rev. C* **47**, R2462 (1993).
- [10] P. G. Blunden and M. J. Iqbal, *Phys. Lett. B* **198**, 14 (1987).
- [11] E. M. Henley and G. Krein, *Phys. Rev. Lett.* **62**, 2586 (1989).
- [12] T. Hatsuda, H. Høgaasen, and M. Prakash, *Phys. Rev. Lett.* **66**, 2851 (1991).
- [13] T. Schaefer, V. Koch, and G. E. Brown, *Nucl. Phys.* **A562**, 644 (1993).
- [14] M. A. Shifman, A. I. Vainshtein, and V. I. Zakharov, *Nucl. Phys.* **B147**, 385 (1979); **B147**, 448 (1979).
- [15] S. Narison, *QCD Spectral Sum Rules* (World Scientific, Singapore, 1990).
- [16] M. A. Shifman, A. I. Vainshtein, and V. I. Zakharov, *Nucl. Phys.* **B147**, 519 (1979).
- [17] S. A. Coon and R. C. Barrett, *Phys. Rev. C* **36**, 2189 (1987).
- [18] P. C. McNamee, M. D. Scadron, and S. A. Coon, *Nucl. Phys.* **A249**, 483 (1975); S. A. Coon and M. D. Scadron, *ibid.* **A287**, 381 (1977).
- [19] R. P. Feynman, *Photon-Hadron Interactions* (Benjamin, Massachusetts, 1972).
- [20] J. Gasser and H. Leutwyler, *Phys. Rep.* **87**, 77 (1982).
- [21] G. Launer, S. Narison, and R. Tarrach, *Z. Phys. C* **26**, 433 (1984).
- [22] J. Gasser and H. Leutwyler, *Nucl. Phys.* **B250**, 465 (1985).
- [23] S. Narison, *Riv. Nuovo Cimento* **10**, 1 (1987).
- [24] C. A. Dominguez and E. de Rafael, *Ann. Phys.* **164**, 372 (1987).
- [25] S. Narison, *Phys. Lett. B* **216**, 191 (1989).
- [26] N. Paver, Riazuddin, and M. D. Scadron, *Phys. Lett. B* **197**, 430 (1987).
- [27] T. Hatsuda, H. Høgaasen, and M. Prakash, *Phys. Rev. C* **42**, 2212 (1990).
- [28] C. Adami, E. G. Drukarev, and B. L. Ioffe, *Phys. Rev. D* **48**, 2304 (1993).
- [29] V. Gimenez, J. Bordes, and J. Penarrocha, *Nucl. Phys.* **B357**, 3 (1991).
- [30] M. Gell-Mann, R. Oakes, and B. Renner, *Phys. Rev.* **175**, 2195 (1968).